An Enhanced Series-Connected Offshore Wind Farm (SC-OWF) System Considering Fault Resiliency

James Tait, Shuren Wang, *Member, IEEE*, and Khaled H. Ahmed, *Senior Member, IEEE*

***Abstract*—The series-connected offshore wind farm (SC-OWF) is a promising offshore wind generation solution to mitigate the need of centralized offshore high-voltage/power converter stations. Predominantly, researchers have focused on the steady-state operation and control of SC-OWFs, without considering the system-level characteristics and ability to ride-through dc side and ac network faults. This paper proposes an enhanced system for SC-OWF applications with fault-resilient capability, where comprehensive circuit configuration and protection strategies are articulated to minimize the negative effects caused by various types of dc and ac faults. For the offshore wind farm architecture, a grouping scheme is adopted where a substation based on disconnectors and diodes is proposed to realize prompt fault bypass/isolation and protection functions in the event of offshore system faults. Additionally, an onshore fault-tolerant modular multilevel converter (MMC) with modified dc-system-oriented control is employed to enable smooth and secure operation under steady-state and fault conditions. The proposed SC-OWF system is quantitatively substantiated by time-domain simulations where four ac/dc fault cases are considered, and the results consolidate the feasibility of the proposed configuration and control, indicating fault resilience of the SC-OWF system. Additionally, size, weight and cost estimations of the proposed offshore substation are presented and compared to a conventional MMC offshore station, to further highlight the merits of the proposed solution.**

***Index Terms*—Fault resiliency, high-voltage dc (HVDC) transmission, power converters, wind generation.**

I. Introduction

The exploitation of offshore wind resources is seen as a critical pathway to realize low-carbon targets globally whilst an estimated 80 GW of annual installation is required by 2050 [1]. Generally, offshore wind farms (OWFs) located at distances beyond 50–80 km from shore benefit from high-voltage dc (HVDC) technology for bulk transmission, due to technical and commercial constraints associated with conventional ac transmission [2]. SC-OWFs can directly establish HVDC transmission voltage at their offshore terminals, through the output voltage summation of multiple series-connected generation units, thereby negating requirement of centralized offshore HVDC stations with massive size and weight [3].

A plethora of current/voltage source converter topologies have been considered for interfacing wind energy conversion systems (WECSs) with the HVDC-link, including uncontrolled diode rectifiers [4] and pulse width modulation (PWM) based converters [5]–[8]. In addition, high-ratio dc/dc conversion employing medium-frequency transformer (MFT) technologies and robust diodes are implemented to achieve successful trade-offs with high wind turbine level controllability, high operation efficiency, galvanic isolation, reduced mass, etc., for offshore system implementation [9]–[11].

Operational characteristics and requirements of the overall SC-OWF differ from its parallel-connected counterpart. As a means of balancing voltages of the WECSs in series connection, extra circuits may be adopted to either exchange energy between units [12] or employing energy storage [13], which increases costs on power converters. However, the motivation of deploying the additional circuitry is system balancing, instead of enhancing system resiliency against system-wide faults. Coordinated operation between the offshore WECSs and the onshore half-bridge modular multilevel converter (HB-MMC) station (operating in constant dc-link voltage control mode) can also be used to avoid WECS overvoltage issues via communications link [14]. In [15], the voltage sharing between offshore WECSs can be addressed by the HB-MMC which operates in a dc-link current control mode. However, the effectiveness is limited by the dc-terminal voltage range of HB-MMCs under low wind power (thereby dc-link voltage) conditions, and therefore a backup function is usually required to regain dc-link voltage control, leading to non-linear control and operation. Other MMC types with larger dc-terminal voltage ranges, such as the full-bridge MMC (FB-MMC), can be used to facilitate the dc-link current control in the SC-OWF applications [16].

MMCs with dc fault isolation or ride-through capability (such as FB-MMC [16], hybrid MMC [17], and T-type MMC [18]) can be used to protect the onshore system against severe dc-side/offshore faults. Yet, due to topological characteristics, SC-OWFs high fault vulnerability increases the overall system's reliability risk. A salient merit of conventional SC-OWFs is eliminating the requirement of offshore infrastructure [14], however the system security of this configuration is compromised when subject to offshore cable faults (short and open circuits). Offshore grounding faults are studied in [19], where the cascading effect of such faults is highlighted, and a fault-clearance method based on coordinated operation of a specific WECS dc/dc converter and protective switches is given, however, only short-circuit to ground faults are considered in this study. Although dumping resistors (DRs) are deployed within the WECSs to provide wind turbine level protection, any collector cable rupture (open circuit) fault will completely cease the system power transmission [15], resulting in high venerability with long periods of zero power production. Besides, the coordinated regulation of offshore and onshore subsystems in various fault scenarios is not yet determined [20]. Therefore, key operational challenges with SC-OWF systems can be identified as poor power/voltage balancing, low system reliability, and inferior fault management. Conclusively, wide research gaps clearly exist for SC-OWF applications, predominantly on the overall system resiliency against different onshore and offshore faults.

This article has been accepted for publication in IEEE Transactions on Power Delivery. This is the author's version which has not been fully edited and content may change prior to final publication. Citation information: DOI 10.1109/TPWRD.2022.3219373

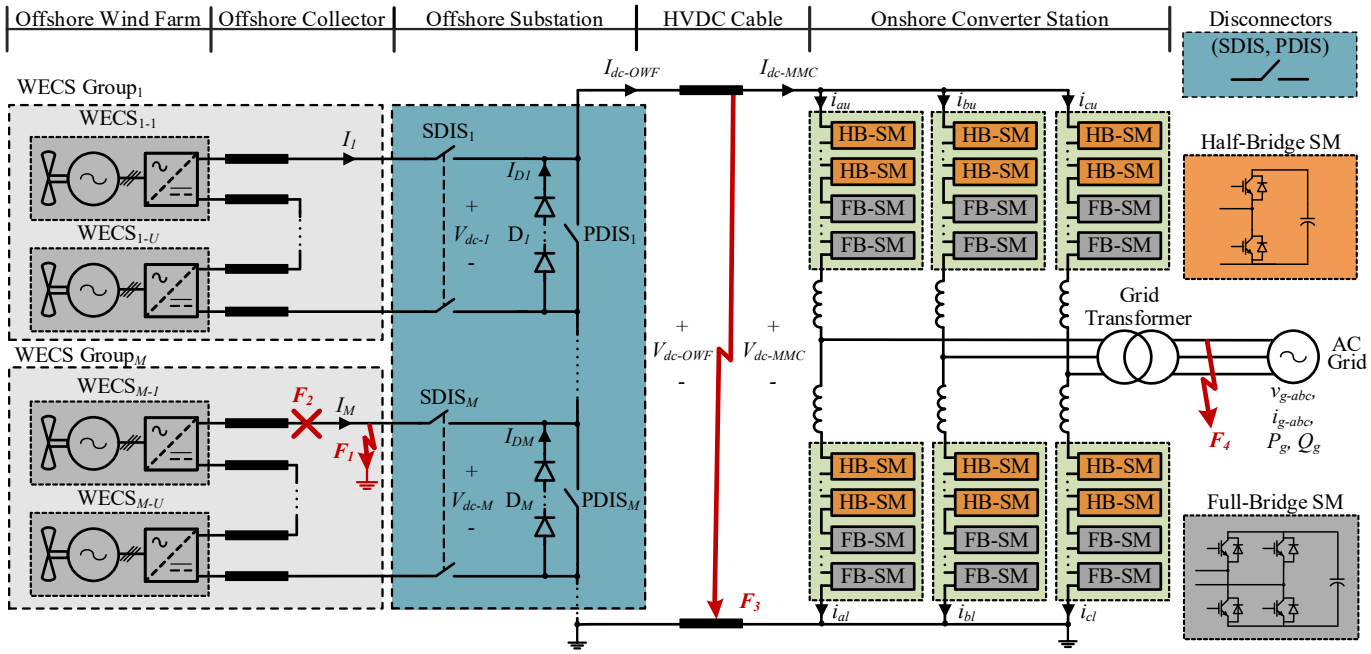

Fig. 1. Architecture of the proposed SC-OWF system.

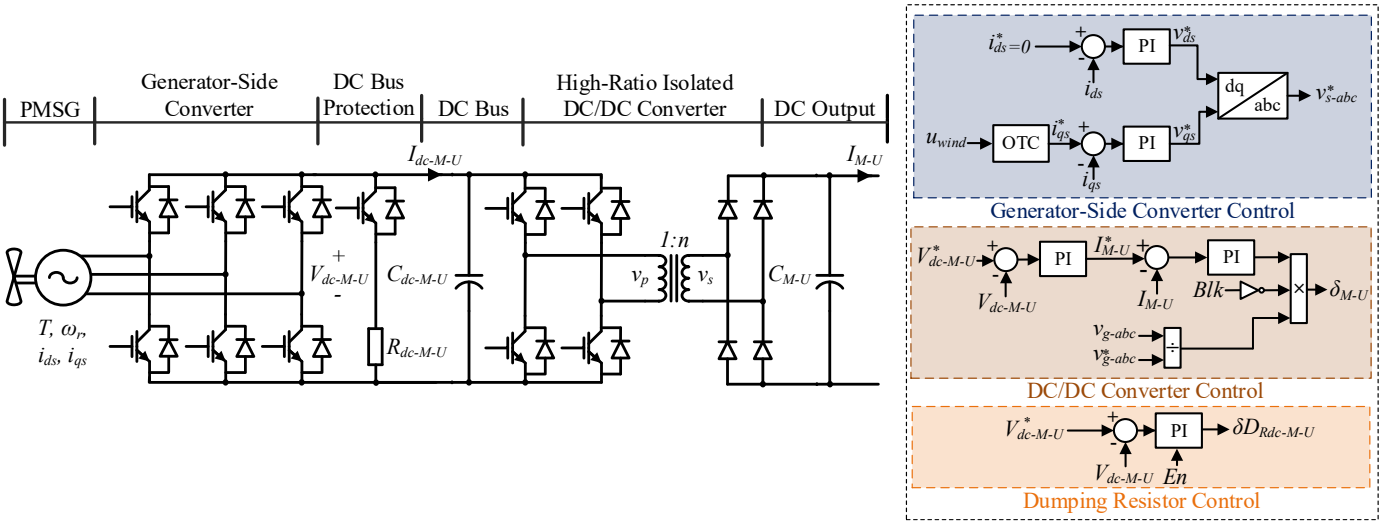

Fig. 2. Schematic diagram and control structure of WECS.

This paper aims to address these challenges and proposes an enhanced system architecture and control structure for SC-OWF applications to improve resilience against multiple types of faults with simple design and low costs. Both offshore and onshore subsystem configurations have been arranged to enable fault-tolerant operation with detailed coordinated control strategies presented. To reduce power losses and simplify power converter design, diode rectifier is adopted as the output stage of each WECS. To maximize the transferrable generation during dc collector faults, series connected WECSs are grouped by additional protective substations, where the combination of disconnectors and protective bypass diodes are employed to enable a reconfigurable offshore network. The proposed protective substation is intentionally deployed on a separate platform within the offshore SC-OWF to provide external current paths, enabling fault ride-through in a simple and cost-effective manner. Importantly, the proposed concept will not require complex and costly dc circuit breakers (DCCBs). The onshore converter station is realized by a dc-fault tolerant MMC equipped with novel control system to maintain key system parameters within tolerable limits in steady-state operation and different fault scenarios. Furthermore, a coordinated approach between the offshore units, onshore MMC system, and the ac grid are included, which allows system-wide secure action during contingencies. The main technical findings of this study are consolidated with simulation verification of four typical fault cases, namely offshore collector short circuit fault, offshore collector open circuit fault, HVDC cable short circuit fault, and asymmetrical ac grid fault. Evaluation and comparison between the proposed offshore substation and an offshore HVDC-MMC station in terms of estimated volume, weight and cost are presented, in order to emphasize the benefits of the proposed substation over the conventional centralized power converter based solution.

The remainder of this paper is structured as follows. Section II details the proposed system architecture, control structure and

operation principles. Section III proposes fault ride-through strategies. A case study including time-domain simulation results and volume, weight and cost assessment is presented in section IV, while conclusions are presented in section V.

II. System Architecture and Control

The proposed SC-OWF system architecture is presented in Fig. 1. The offshore series-connected WECS units are configured into N groups whereas each group consists of U individual units. A total of $N \times U$ WECSs are therefore connected through HVDC cables to an onshore converter station (for example, the hybrid MMC as illustrated) that transfer power into the ac grid. The offshore wind farm configuration can improve system fault resiliency, whilst the onshore station ensures well-regulated operation in both normal and fault cases.

Each of the following subsections details the major elements of the proposed system in terms of configuration and control.

A. Wind Energy Conversion System (WECS)

In general, the applicable WECS configurations and topologies vary, whereas the conversion stages and technologies aligning with those in [14] are adopted herein, as presented in Fig. 2. In general, dimensions of the permanent magnet synchronous generator (PMSG) can vary with the overall SC-OWF setup, where both low and medium voltage variants would be applicable [11], [12], [21], [22]. The PMSG side ac/dc conversion stage employs IGBT switches, thereby being advantageous in terms of controllability and ripple propagation [9]. The active energy dissipation device, assumed to be a DR, is employed within dc bus protection stage, as per [23]. The galvanic isolation of the WECS is of significant importance and can be achieved by an air core MFT with the aim of reducing mass and losses [22]. The high transformation ratio of the proposed dc/dc conversion stage has been proposed in [24] and will be applied herein. Fig. 2 presents the dc/dc converter as an aggregated system for simplicity where a practical system may adopt a modular topology presented in [21], using one or more IGBT active bridges driving one or more MFTs within a rectification stage. Compared with controlled output rectifier stages in [11], [13], [19], the proposed diode rectification stage features relatively low capital costs and operational losses, and simple converter design, which is especially beneficial for such applications requiring galvanic isolation and high-voltage ratings.

Considering a generic WECS (like the U^{th} of the M^{th} group), the generator-side control ensures wind power injection into the dc bus based on wind speed. The dual-loop dc/dc converter control regulates the dc bus voltage ($V_{dc\text{-}M\text{-}U}$), therefore the WECS output dc voltage $V_{M\text{-}U}$ varies depending on the available wind power, affecting the total offshore string output voltage (assuming a controlled and constant dc-link current) [21]. Importantly, inter-WECS voltage balancing is not challenging in such a system with single string offshore WECSs, controlled dc-link current and the maximum WECS output voltage would be the rated [15]. A blocking signal *Blk* (equal to 1 in steady-state) will be used in fault cases, $Blk = 0$ is applied to block power transfer with the diode rectification bridge entering in a freewheeling state. During contingency periods, the DR devices will maintain dc bus voltage ($V_{dc\text{-}M\text{-}U}$) within limits, thereby mitigating PMSG electromechanical stresses. The control structure of the DR is shown in Fig. 2, where the PI controller is enabled during contingency periods via the *En* port. Furthermore, the control setpoint is configured to be marginally higher than the rated dc-bus voltage, so that during contingencies the additional energy can be consumed without interfering with steady-state operation. To allow for prompt de-loading (energy balancing) during the onshore ac grid faults, a coordination mechanism via high-speed communication is included between the offshore WECSs and the onshore integrated grid, as shown in Fig. 2. In steady-state operation, the grid voltage is at approximately nominal value ($V_{g\text{-}abc} = 1$ pu); thus, there is no reliance on the communication mechanism during normal operation. When a grid fault occurs, the dc/dc converter duty cycle ($\delta D_{M\text{-}U}$) can be altered based on the onshore grid voltage magnitude ($V_{g\text{-}abc}$), which allows reduction of the WECSs' generation contribution to the HVDC-link, thereby effectively maintaining system power balance. In extreme cases, (e.g., simultaneous communication failure and onshore grid fault), the WECS DR and MMC local protection (as per [25]) can still ensure the system to be maintained within tolerable limits. Such manipulation of WECS energy contribution can be used for more advanced system management such as frequency containment reserve depending on system operators.

B. WECS Grouping Configuration and Offshore Substation

In the proposed system, each of the WECS groups is interfaced into the HVDC system (e.g., group M) via a two-pole series disconnector (SDIS_M), a parallel disconnector (PDIS_M) and diode unit(s) (D_M), as shown in Fig. 1 (relevant auxiliary protective components such as surge arresters are omitted for simplicity). Conventional SC-OWFs have no external current path apart from the series-connected wind turbines, where a single wind farm section fault will be cascaded, thereby affecting overall power export. Also, to isolate the fault, the entire system must be isolated. In contrast, the proposed WECS grouping arrangement, which employs a separate offshore substation, can provide external current paths in parallel with the wind turbines. The selection of numbers of groups and WECSs within the group involves many factors such as device manufacturing capacity, cable failure probability, design complexity, cost, engineering factors, etc. In terms of functionality, the SDIS is used to isolate the WECS group, where the PDIS ensures bypass of the group for long-term periods (e.g., fault isolation or normal maintenance). The substation can be a common bus array with reasonable isolation and insulation margins, thereby minimizing susceptibility of internal faults. The grouping method allows the diode strings and PDISs to be rated to the group nominal voltage; whereas the voltage ratings of the SDISs can vary depending on the group position within the string (lower the position, lower the rating), leading to a positive effect on the choice of component ratings and space requirements practically [28]. The additional offshore substation introduces greater flexibility and enables circuit manipulation during SC-OWF faults. Also, this design eliminates the requirement for complex and costly dc circuit breakers (DCCB), with detailed operation during offshore system faults given in section III.

This article has been accepted for publication in IEEE Transactions on Power Delivery. This is the author's version which has not been fully edited and content may change prior to final publication. Citation information: DOI 10.1109/TPWRD.2022.3219373

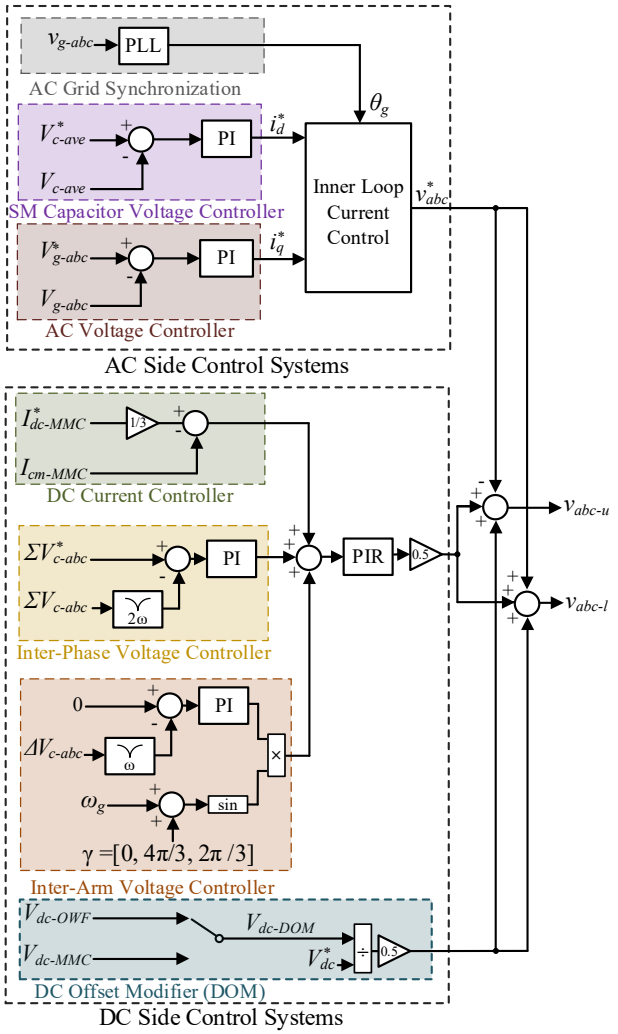

Fig. 3. Control structure of the onshore MMC station.

C. Onshore Converter Station

The onshore converter station can be implemented by MMCs with the dc fault ride-through (zero dc-side voltage operation) capability [26], such as topologies equipped with sufficient full-bridge submodules (FB-SMs) as shown in Fig. 1 [3], [16].

The MMC control system is critical to maintain system security within tolerable limits during steady-state operation and faults, whereas the proposed MMC control is shown in Fig. 3. In this paper, the grid-connected control system is designed and operated based on grid-following strategy through the implementation of a phase-lock loop (PLL) that generates a grid angle reference (θ_g) [27]. Given that the onshore MMC station is a voltage source converter type, it can be anticipated that potential grid-forming control schemes are also applicable. The MMC ac side *d-q* current control references are regulated by average capacitor voltage controller and grid voltage (or reactive power) controller respectively, analogous to [28]. The dc-link current control is achieved by regulating MMC common mode current ($I_{cm\text{-}MMC}$); the reference can be optimized for low power operation in low wind or contingent cases, which allows the dc-link voltage regulation down to zero [15]. To maintain the balance of capacitor voltages within the MMC, correction signals for inter-phase and inter-arm capacitor balancing are implemented. Outputs of dc current, inter-phase voltage and inter-arm voltage controllers are fed into the proportional-integral-resonant (PIR) controller [29]. Importantly, to effectively maintain onshore and offshore power balance in both steady-state and abnormal cases, a dc offset modifier (DOM) is adopted, shown in Fig. 3. The MMC dc-terminal voltage can be promptly adjusted with the offshore dc voltage ($V_{dc\text{-}OWF}$) through high-speed communications (a minor delay in ms level is tolerated for both sides). Unlike other proposals utilizing current control methods [21], [30], the DOM inherently responds to wind variations, adjusting the MMC dc-terminal voltage, while maintaining rated dc-link current without leading to energy curtailment. Importantly, the DOM can also accept locally measured MMC dc-terminal voltage ($V_{dc\text{-}MMC}$), acting as suitable system redundancy in the event of potential communication failures. Therefore, a universal linear control scheme can be realized in normal and fault scenarios without switching between different control modes.

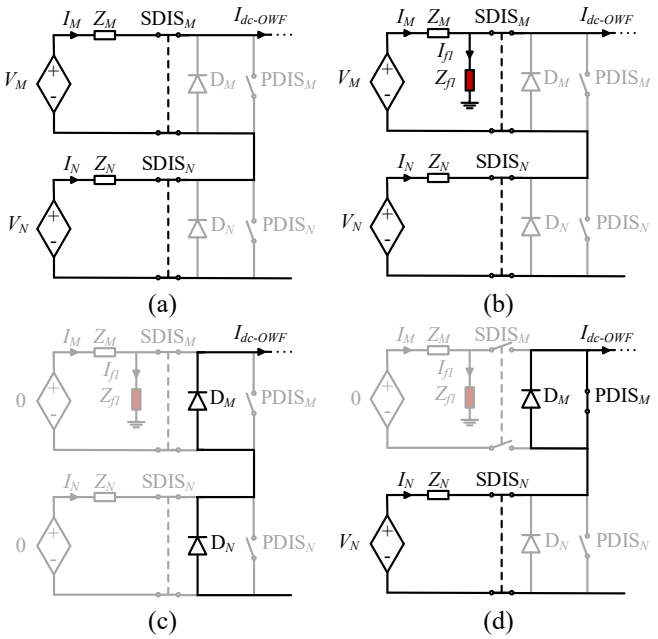

Fig. 4. Equivalent circuits of SC-OWF section in F_1 fault case. (a) Steady-State operation. (b) Fault occurrence at group *M*. (c) Fault condition with ceased power transfer of groups *M* and *N*. (d) Bypass and isolation of the faulty group *M*.

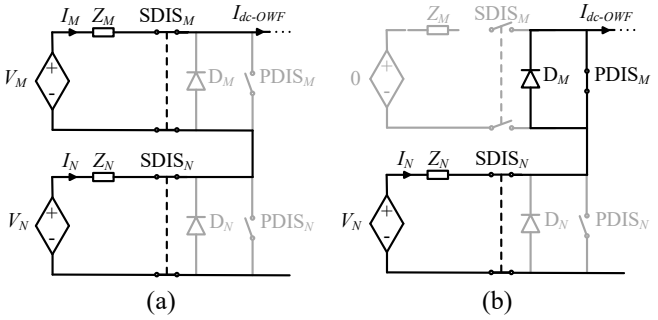

Fig. 5. Equivalent circuit of SC-OWF section in F_2 fault case. (a) Steady-State operation (b) Bypass and isolation of the faulty group *M*.

III. System Fault Ride-Through Strategy

System fault management and power transmission reliability are critical for the SC-OWF systems. This section articulates operational behavior and fault ride-through strategies of the proposed SC-OWF system considering four fault types, which are highlighted in Fig. 1, as follows:

- *F_1: Offshore Collector Cable Short Circuit Fault*
- *F_2: Offshore Collector Cable Open Circuit Fault*
- *F_3: HVDC Cable Short Circuit Fault*
- *F_4: AC Grid Fault*

The studied faults comprehensively represent typical cases that occur within the SC-OWF system, with common causes attributed to insulation degradation (short circuit), external aggressors (open and short circuit) and mechanical fatigue at termination points (open circuit) [31].

A. F_1: Collector Cable Short Circuit Fault

Conventionally, SC-OWFs are inherently susceptible to offshore side faults with cascading effects. A cable to ground short circuit fault at the offshore collector affects the power transfer of all WECSs units connected within the string, potentially leading to a system shutdown and lasting for prolonged durations. Such revenue losses can be significantly minimized by employing the proposed system with WECS units, grouping philosophy and offshore substation.

Assuming the F_1 fault occurs at the first WECS unit of the group M, Fig. 4 shows an equivalent representation of an SC-OWF section configured into groups M and N, each containing U WECSs. In steady-state operation, as shown in Fig. 4(a), the section output voltage is determined by the voltage sum of groups M and N ($V_M + V_N$) and string current $I_{dc\text{-}OWF}$ is regulated by onshore MMC. Fig. 4(b) depicts the section behavior when a grounding fault (with impedance of Z_{f1}) occurs to the upper side collector of group M, this cascades to both groups through the fault conduction path to earth. After the fault occurs, both WECS groups can effectively stop power contribution with their output voltage regulated to zero (the blocking signal Blk = 1 is issued, with surplus power from the generators consumed by WECS local DRs). With groups M and N ceasing their power contribution, fault currents decay within the duration which is mainly dependent on the total damping resistance in the fault loop. Furthermore, the dc current is transferred from the WECS units to the diode units D_M and D_N situated at the offshore substation, as per the circuit shown in Fig. 4(c). Simultaneously, power balancing between the onshore and offshore sides is maintained mainly by the DOM mechanism of the onshore MMC, where MMC dc-terminal voltage $V_{dc\text{-}MMC}$ and ac power P_g are reduced based on the available SC-OWF group capacity.

With the current flow through $SDIS_M$ reduced to an acceptable level, $SDIS_M$ can be opened to eliminate residual current and achieve fault isolation; meanwhile, SC-OWF current flows through D_M. Blocking signals of group N WECSs can be cleared (Blk = 0), allowing output voltage restoration and power transfer recovery. In addition, $PDIS_M$ can be closed to achieve long-term isolation of the fault from the system. Fig. 4(d) shows the SC-OWF section with group M isolated and the system retains operation with group N. Additionally, the onshore MMC dc voltage should be decreased correspondingly to allow reduced power transfer, whilst dc-link current can be maintained. This configuration eliminates the requirement for DCCBs and allows WECS units connected below group M in the string to retain long-term operation, thereby greatly improving system resiliency. The generation degradation level mainly related to grouping configuration/numbers.

B. F_2: Collector Cable Open Circuit Fault

Open circuit faults result in a full power transmission loss, potentially for prolonged durations, which poses a serious reliability concern for conventional SC-OWFs. By applying the proposed offshore substation equipped with diode-based bypassing capability, offshore collector open circuit faults can be promptly managed, allowing power production to continue.

Fig. 5(a) shows the steady-state configuration of the SC-OWF represented by two groups M and N. At the occurrence of the fault, WECSs contained in group M will cease power transfer and extra energy will be consumed by its DR. Simultaneously, D_M becomes forward-biased and conducts dc-link current. As the transmitted power is reduced, the onshore MMC, via DOM, can be manipulated to reduce $V_{dc\text{-}MMC}$ in an effective manner, with dc-link current control maintained at the operational setpoint.

As no current presents in group M, $SDIS_M$ can be opened to isolate the fault from the network; $PDIS_M$ can be closed to ensure a safe bypass path and gain lower losses. Fig. 5(b) shows the network condition where the normal dc-link current can flow through D_M (predominantly $PDIS_M$, if closed) allowing the smooth operation of group N. By implementing the offshore substation configuration with the coordinated control, system resiliency is enhanced against the collector open circuit faults.

C. F_3: HVDC Cable Short Circuit Fault

The SC-OWF system is required to safely ride-through HVDC cable faults, which pose high risk to device safety and power transmission similar to other HVDC systems.

As shown in Fig. 1, at the occurrence of a dc-link fault, the system is split into two major circuitry loops (by the short circuit point). The WECSs are blocked (Blk = 1) to cease power transfer (with surplus power generation dissipated by DRs). Current within the offshore loop will begin to decay at a rate corresponding to the total loop damping resistance. Meanwhile, onshore the MMC fault blocking capability is activated, to effectively reduce MMC dc terminal voltage, maintain SM capacitor voltage, and regulate $I_{dc\text{-}MMC}$ to zero (export power P_g is stopped). In addition, the MMC can still deliver reactive power, if required, operating in static compensation mode.

D. F_4: AC Grid Fault

Generally, grid code regulations specify the fault severity and duration to which wind farm systems are expected to remain connected to the ac network to ensure system security and stability. The key challenge of the SC-OWF is to address power transfer coordination between onshore and offshore units herein as the ac power transfer is limited/eliminated.

By employing an ac voltage signal to the offshore WECSs, overall system power management is achieved in a coordinated manner, even extending to ac grid disturbances. After a short communication period in ms, the WECSs output is reduced proportionally with the grid voltage magnitude, with surplus WECS energy consumed by DRs. The MMC dc-terminal

This article has been accepted for publication in IEEE Transactions on Power Delivery. This is the author's version which has not been fully edited and content may change prior to final publication. Citation information: DOI 10.1109/TPWRD.2022.3219373

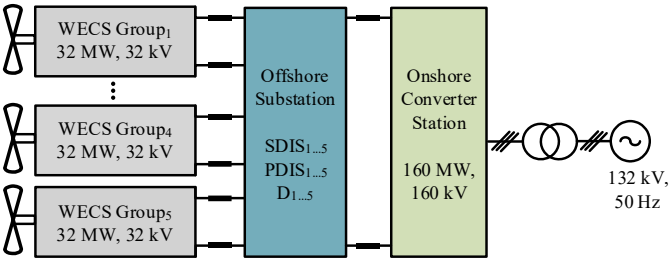

Fig. 6. Schematic diagram of simulated SC-OWF system.

TABLE I
CASE STUDY SYSTEM PARAMETERS

	Items	Values
Offshore WECSs	Wind turbine rotor diameter (D)	167 m
	Rated power per WECS unit	8 MW
	PMSG rated (rms) voltage	0.69 kV
	WECS dc bus rated voltage	1.2 kV
	WECS dc bus capacitance	110 mF
	WECS IGBT switching frequency	1 kHz
	WECS dc output rated voltage	8 kV
	WECS dc output capacitance	2.5 mF
	SC-OWF WECS group No. (N)	5
	WECS units No. per group (U)	4
	Total WECS No. ($N \times U$)	20
Offshore Substation	Total No. of diodes (D2601NH90T)	40
	Total No. of SDISs	10
	Total No. of PDISs	5
Offshore Collectors & Cables	Distance between 2 adjacent WECSs	1.2 km
	Total cables No. per group	5
	Total cable length per group	6 km
	HVDC cable length	40 km
	Cable resistance	35 mΩ/km
	Cable inductance	1 mH/km
	Cable capacitance	0.172 μF/km
Onshore Converter Station	Rated power capacity	160 MVA
	Rated dc voltage	160 kV
	Total MMC SM No. per arm	80
	MMC HB-SM No. per arm	40
	MMC FB-SM No. per arm	40
	MMC SM capacitance	8 mF
	MMC SM rated voltage	2 kV
	MMC arm inductance	28.6 mH
AC Grid	Interfacing transformer ratio	1:1.47
	Interfacing transformer leakage	0.2 pu
	Frequency	50 Hz
	Rated (rms) voltage	132 kV

voltage is adjusted in a dynamic way through DOM mechanism, inherently responding to the offshore voltage reduction, with the dc-link current maintained.

IV. CASE STUDY BASED VERIFICATION

This section details study cases and results based on MATLAB/Simulink simulation of the proposed SC-OWF system, as illustrated in Fig. 6. In addition, estimated volume, mass and cost of an offshore HVDC-MMC station and the proposed offshore substation are assessed and compared.

Table I lists key system parameters utilized for system modeling, where the system architecture and control are configured as presented in section II. In this case study, low-voltage (0.69 kV) PMSGs are adopted, which align with commercial products [32]–[34]. The wind turbine properties are assumed to be extrapolated based on [35]. The cable distance between two adjacent wind turbines within one group is assumed to be 7D, while detailed sub-siting/sub-string arrangements are not considered herein [36]. Also, a multi-section π-model is used to represent dc cables in the simulation, which aligns with [19], [37]. The four types of faults (detailed in Section III) are applied with 1 ms fault detection duration and communication delay between onshore and offshore sides is applied for all cases. All studied faults are assumed to be

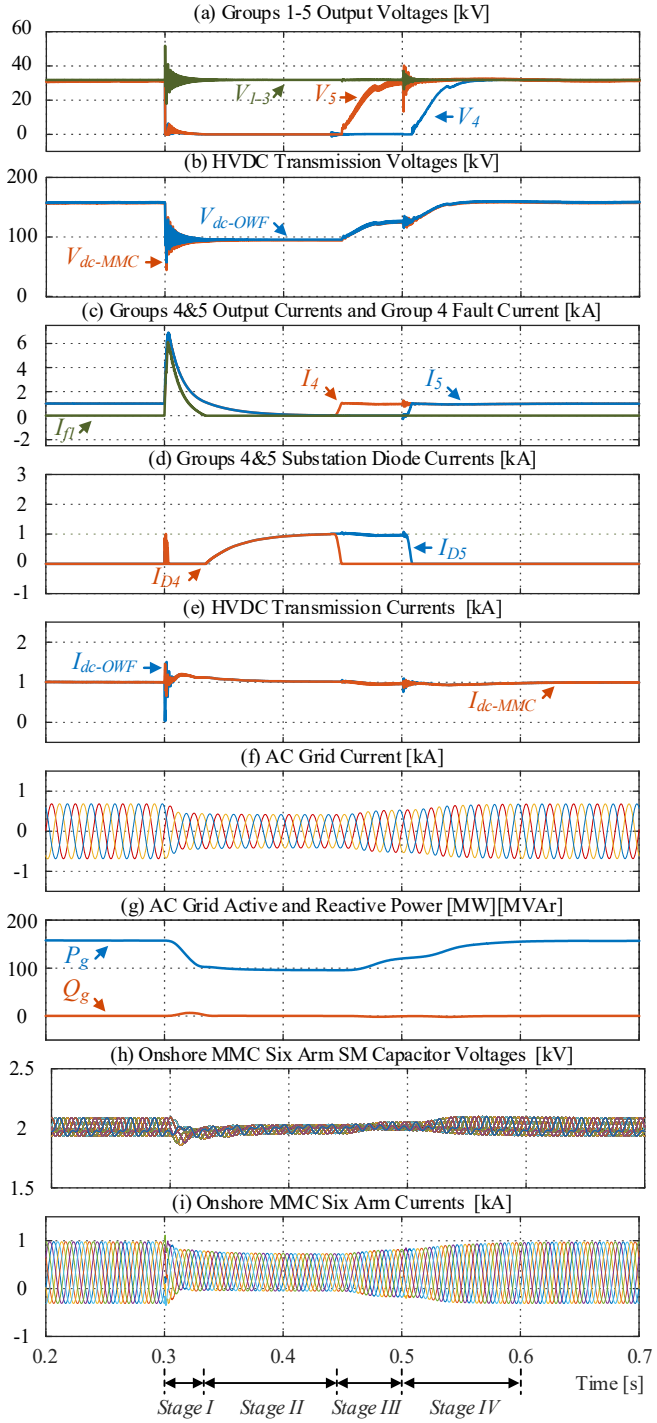

Stage I: Fault occurs and Groups 4&5 power transfer ceased
Stage II: Bypass path established through D_4 and D_5
Stage III: Fault isolated, Group 5 power transfer resumes
Stage IV: Fault cleared and Group 4 power transfer resumes

Fig. 7. Simulation results of collector cable short circuit fault (F_1) case at group 4.

This article has been accepted for publication in IEEE Transactions on Power Delivery. This is the author's version which has not been fully edited and content may change prior to final publication. Citation information: DOI 10.1109/TPWRD.2022.3219373

temporary from 0.3 s to 0.5 s in order to include system recovery performance. The onshore station operates with 1 pu active power injection at unity power factor.

A. Collector Cable Short Circuit Fault (F_1) Case

A short circuit fault (F_1) is applied at the uppermost collector cable of group 4 with groups 1 to 3 above and group 5 below in the string (both of which are normal/healthy). Simulation results of this case are presented in Fig. 7, with the 1 Ω impedance fault applied between 0.3 s and cleared at 0.5 s.

With the occurrence of F_1, the SC-OWF cascading nature leads to initial voltage collapses of groups 4 and 5 (V_4 and V_5), with groups 1 to 3 voltages ($V_{1\text{-}3}$) remaining at the pre-fault output (32 kV per group), as shown in Fig. 7(a), where the overvoltage surges can be absorbed by protective devices practically. Simultaneously, the output current of group 4 (I_4), and currents of WECS group 5 and its substation diode unit (I_5 and I_{D5}) rise in different dynamics due to the fault current flow and different cable impedances, as shown in Fig. 7(c). Shortly after detecting the fault, WECSs of groups 4 and 5 are blocked (with Blk = 1 triggered) and group output currents begin to decrease due to the stray resistive impedance within the fault loop (Stage I). Substation diode units D_4 and D_5 begin to conduct the current at about 0.34 s, as shown in Fig. 7(c) and (d), indicating that there is an increasing amount of current to be carried by groups 4 and 5 bypass diode units within the offshore substation (Stage II). Therefore, as groups 1 to 3 remain connected (as main offshore power contributors), offshore overall output voltage $V_{dc\text{-}OWF}$ reduces to 96 kV and dc-terminal voltage of the onshore MMC $V_{dc\text{-}MMC}$ is promptly reduced, through the proposed DOM mechanism, as shown in Fig. 7(b). Also, the dc-link current $I_{dc\text{-}MMC}$ is maintained by the MMC control system during the fault, see Fig. 7(e). The active power injected into the grid P_g is reduced correspondingly to be 96 MW, as shown in Fig. 7(f) and (g). Throughout the fault duration, the MMC SM capacitor voltages and arm currents are regulated within acceptable limits, as shown in Fig. 7(h) and (i) respectively.

The proposed system can retain the normal/healthy group 5 back into the generation mode with a successful current commutation. At approximately 0.44 s (Stage III), D_4 and D_5 are carrying sufficient dc current share, allowing group 4 series-connected disconnector ($SDIS_4$) to be safely opened, thereby isolating the faulty section (group 4). WECSs of group 5 can resume power transfer into the HVDC system by re-establishing its output voltage ($Blk = 0$). The development of V_5 includes an acceptable stabilizing period due to control system, which allows the increase of $V_{dc\text{-}MMC}$ and thus P_g (to be about 128 MW), with I_{D5} current nullified. This action maximizes wind power generation of available/normal WECSs in long term operation.

If F_4 is cleared (at 0.5 s), $SDIS_4$ can be closed and WECSs of group 4 can restore back to the generation mode (Blk = 0), facilitating a smooth power recovery to the pre-fault value at about 0.6 s (Stage IV).

B. Collector Cable Open Circuit Fault (F_2) Case

Fig. 8 shows system performance with a collector cable open circuit fault (F_2) located at the uppermost cable of group 4.

At 0.3 s, group 4 power contribution to the HVDC system is stopped, resulting in the elimination of output voltage (V_4) and current (I_4), as shown in Fig. 8(a) and (c). During the fault, the offshore substation diode D_4 becomes forward-biased to promptly establish a conduction path for the offshore dc current ($I_{dc\text{-}OWF}$), and group 4 energy production is consumed locally by WECS DRs, as shown in Fig. 8(c) and (d). Simultaneously, the healthy group voltages $V_{1\text{-}3}$ and V_5 remain at the pre-fault values, subsequent to a short oscillation/surge period, caused by circuit interruption (which can be suppressed by protective devices), as shown in Fig. 8(b). Offshore dc-link voltage is reduced (to be 128 kV), where onshore MMC reacts quickly via the DOM mechanism, with dc-link current regulated, as shown in Fig. 8(b) and (d). The MMC avoids power elimination risks, with regulated ac current and reduced active power of about 128

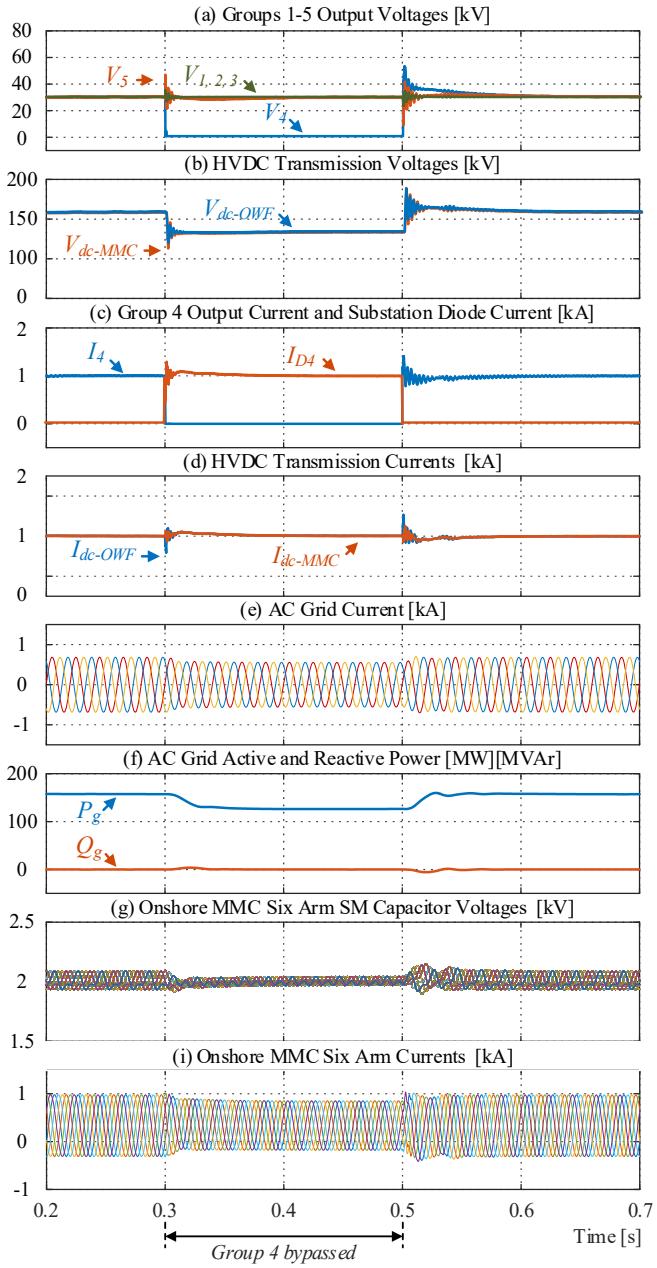

Fig. 8. Simulation results of collector cable open circuit fault (F_2) case at group 4.

This article has been accepted for publication in IEEE Transactions on Power Delivery. This is the author's version which has not been fully edited and content may change prior to final publication. Citation information: DOI 10.1109/TPWRD.2022.3219373

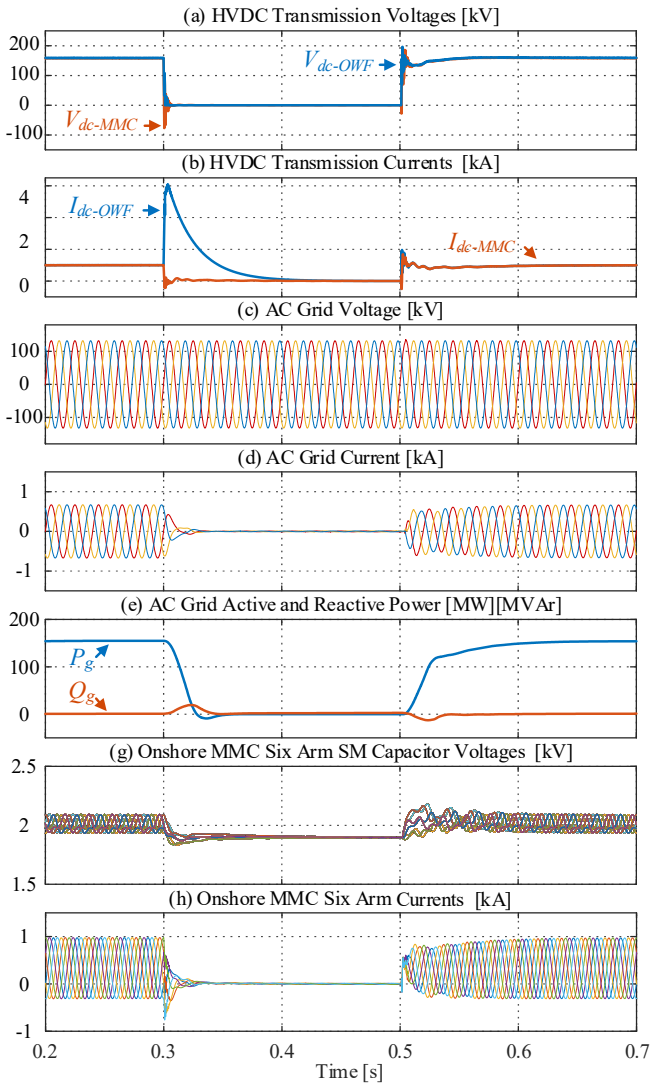

Fig. 9. Simulation results of HVDC cable short circuit fault (F_3) case.

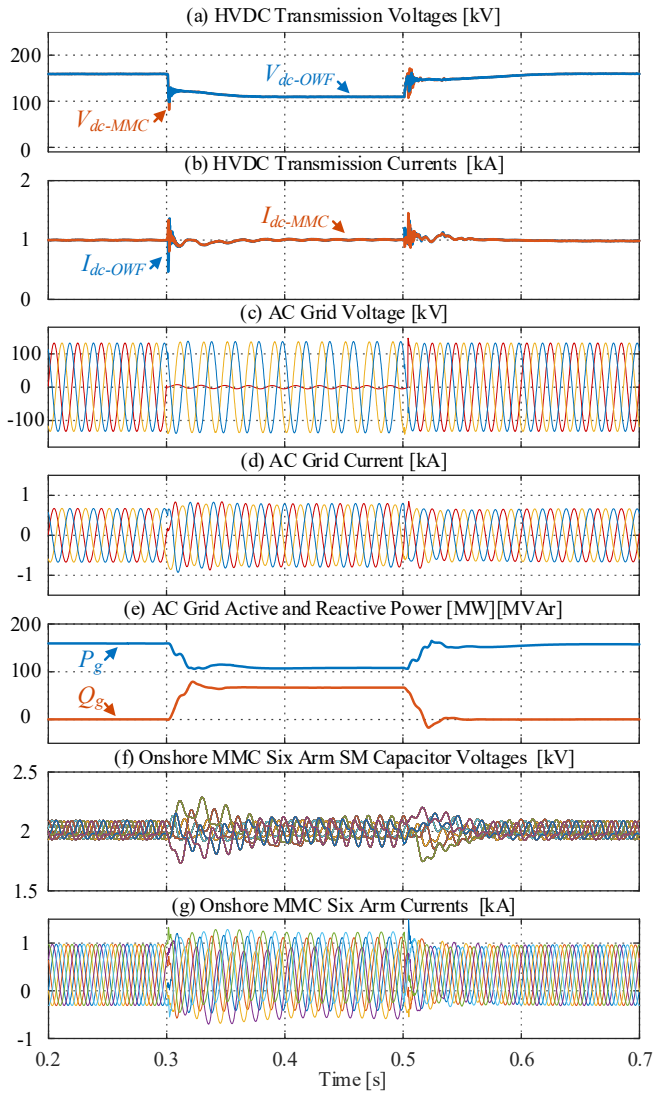

Fig. 10. Simulation results of asymetrical ac grid fault (F_4) case.

MW, see Fig. 8(e) and (f). Throughout the fault, the MMC SM capacitor voltages and arm currents are maintained within acceptable operational limits, see Fig. 8(g) and (h).

After the fault clearance at 0.5 s, group 4 power production can be restored, allowing smooth system recovery back to nominal power transfer at 0.55 s. For a permanent fault, group 4 series and parallel disconnectors ($SDIS_4$ and $PDIS_4$ respectively) can be opened and closed, respectively.

C. *HVDC Cable Short Circuit Fault (F_3) Case*

Fig. 9 shows system performance during an HVDC cable short circuit fault (F_3), which is assumed to be located at 20 km from the onshore substation with 1 Ω impedance.

At 0.3 s, the total offshore voltage $V_{dc\text{-}OWF}$ reduces sharply with $V_{dc\text{-}MMC}$ aligning promptly due to the DOM mechanism, shown in Fig. 9(a). The offshore current $I_{dc\text{-}OWF}$ rises to a peak value of approximately 4.2 kA (shortly, tolerated by diodes), and begins to decrease at a rate determined by the damping resistance of the cable impedance after blocking the WECSs (Blk = 1, and excess energy is dissipated by WECS DRs), as shown in Fig. 9(b). The MMC reference current $I^*_{dc\text{-}MMC}$ is set to 0 shortly and therefore holds $I_{dc\text{-}MMC}$ (offshore fault loop) to 0 A. The onshore ac grid currents and MMC arm currents become zero in this case, as shown in Fig. 9(d) and (g), and the active power transfer ceases, see Fig. 9(e). A minor discharge of SM capacitor voltages occurs to be about 1.9 kV, but is stopped quickly, as shown in Fig. 9(f), indicating the brief period of the detection delay and fault blocking.

At 0.5 s, the fault is cleared and the WECS blocking signal (Blk = 0) can be removed. Group terminal voltages can be established to allow recovery of $V_{dc\text{-}OWF}$ and $V_{dc\text{-}MMC}$, which also enables smooth MMC active power injection recovery.

D. *AC Grid Fault (F_4) Case*

Simulation results in Fig. 10 show system behavior in an asymmetrical (single-phase to ground) ac grid fault (F_4) case, where one phase voltage is collapsed as shown in Fig. 10(c).

At the occurrence of the fault, offshore WECS units respond proportionally to the V_g, effectively de-loading the with $V_{dc\text{-}OWF}$ becoming about 106 kV, as shown in Fig. 10(a), where the undeliverable WECSs power is consumed by local DRs. Through the DOM mechanism, $I_{dc\text{-}OWF}$ and $I_{dc\text{-}MMC}$ are maintained at 1 kA with minor oscillation, as shown in Fig. 10(b). During the fault, ac grid current i_{abc} is controlled at

TABLE II
VOLUME, MASS & COST COMPARISON

Items	HVDC-MMC Station	Proposed Substation
Power [MW]	160	160
Volume [m^3]	8640	92
Weight [tonne]	300	7.7
Cost [$]	18400k	394k

1.2 pu, as shown in Fig. 10(d). The power injection from the MMC into the grid is about 106 MW, where the MMC also injects about 56 MVAr reactive power to regulate the grid voltage depression, see Fig. 10(e). MMC SM capacitor voltages range between 1.8 kV to 2.2 kV shortly after a control stabilization period, whereas the arm currents remain controlled and within the limits, as shown in Fig. 10(f) and (g).

After the grid fault is cleared, grid voltage is re-established, allowing the onshore MMC to inject the rated power, therefore the offshore SC-OWF retain power recovery with $V_{dc\text{-}OWF}$ and $V_{dc\text{-}MMC}$ (via DOM) restored.

E. Offshore Substation Volume, Weight and Cost Analysis

This subsection assesses estimated volume, weight and cost in order to give a comparison between the proposed substation and an offshore HVDC-MMC station.

The estimation of the proposed substation can be achieved by considering diodes and disconnectors, with reasonable margins included. For the selected diode unit (D2601NH90T), volume, mass and cost are estimated to be 0.05 m^3/pcs, 5 kg/pcs and 3k $/pcs respectively, considering auxiliary circuits, heat sinks, etc. Therefore, for the 160 MW system of the studied case, the size, weight and cost of 40 diode units within the proposed substation are 2 m^3, 200 kg and $120k respectively. For the sake of generality and simplicity, it is assumed that disconnectors are the same for different groups, with each dimension and weight being 6 m^3 and 500 kg respectively [38], where margins are included for spacing between units [39]. Also, the mechanical switch cost can be estimated at 570 $/MW [40]. Thus, 15 disconnectors of the proposed substation require approximately 90 m^3, 7500 kg and $274k respectively.

For an MMC-HVDC offshore substation, per MW parameters can be used due to the existence of commercial available projects, namely, volume of 54 m^3/MW, mass (electrical equipment) of 1,875 kg/MW and cost of 115k $/MW approximately [41]–[44].

Comparatively, Table II shows the estimated values of an assumed offshore HVDC-MMC station and the proposed offshore substation (same power ratings are assumed as the studied case). The physical parameters and cost of the proposed offshore substation are significantly lower, where the volume, weight and cost count for approximately 1.1%, 2.6%, and 2.1% of an offshore HVDC-MMC station, showing a very competitive solution for offshore wind integration.

V. CONCLUSION

This paper proposed a series-connected offshore wind farm (SC-OWF) system with novel architecture and control, which prioritize, thus enhance, resiliency against typical faults of high severity. The proposed offshore substation arrangement and manipulation strategies allow the series-connected wind energy converter systems (WECSs) to be electrically grouped, achieving effective fault isolation/bypassing and reducing the risks of permanent generation loss. Also, offshore network complexity and costs are low, through the collective implementation of the WECSs with diode rectifier output stage and the offshore substation utilizing diodes and disconnectors. The onshore subsystem employs a dc-fault-tolerant modular multilevel converter (MMC) with constant dc current control and a dc offset modifier (DOM) mechanism, which can maximize power generation during normal operation and ensure transmission system safety during dc/ac faults. System behavior in four typical dc/ac fault cases were presented, indicating the operational effectiveness. The proposed system can eliminate the requirement of massive offshore converter stations with significantly reduced size, weight and cost, which was confirmed by a comparative estimation between an offshore MMC station and the proposed system. The proposed SC-OWF system would be applicable for future offshore wind generation applications.

REFERENCES

[1] Global Wind Energy Council, "Global offshore wind report 2021," 2021. [Online]. Available: www.gwec.net

[2] E. Apostolaki-Iosifidou, R. Mccormack, W. Kempton, P. Mccoy, and D. Ozkan, "Transmission design and analysis for large-scale offshore wind energy development," IEEE Power and Energy Technology Systems Journal, vol. 6, no. 1, pp. 22–31, Feb. 2019, doi: 10.1109/jpets.2019.2898688.

[3] M. Pape and M. Kazerani, "A generic power converter sizing framework for series-connected dc offshore wind farms," IEEE Trans Power Electron, vol. 37, no. 2, pp. 2307–2320, Feb. 2022, doi: 10.1109/TPEL.2021.3106578.

[4] R. J. Thomas, A. G. Phadke, and C. Pottle, "Operational characteristics of a large wind-farm utility system with a controllable ac/dc/ac interface," IEEE Transactions on Power Systems, vol. 3, no. 1, pp. 220–225, 1988, doi: 10.1109/59.43202.

[5] M. Popat, B. Wu, F. Liu, and N. Zargari, "Coordinated control of cascaded current-source converter based offshore wind farm," IEEE Trans Sustain Energy, vol. 3, no. 3, pp. 557–565, 2012, doi: 10.1109/TSTE.2012.2191986.

[6] E. Veilleux and P. W. Lehn, "Interconnection of direct-drive wind turbines using a series-connected dc grid," IEEE Trans Sustain Energy, vol. 5, no. 1, pp. 139–147, Jan. 2014, doi: 10.1109/TSTE.2013.2276616.

[7] P. Hu, R. Yin, B. Wei, Y. Luo, and F. Blaabjerg, "Modular isolated LLC dc/dc Conversion system for offshore wind farm collection and integration," IEEE J Emerg Sel Top Power Electron, vol. 9, no. 6, pp. 6713–6725, Dec. 2021, doi: 10.1109/JESTPE.2021.3062677.

[8] L. Li, B. Li, Z. Wang, M. Yang, and D. Xu, "Monopolar symmetrical dc-dc converter for all dc offshore wind farms," IEEE Trans Power Electron, vol. 37, no. 4, pp. 4275–4287, Apr. 2022, doi: 10.1109/TPEL.2021.3125095.

[9] Y. Xia, K. H. Ahmed, and B. W. Williams, "A PWM current source-based DC transmission system for multiple wind turbine interfacing," IEEE J Emerg Sel Top Power Electron, vol. 2, no. 4, pp. 784–796, 2014.

[10] Q. Wei, B. Wu, D. Xu, and N. R. Zargari, "Further study on a PWM current-source-converter-based wind energy conversion system considering the dc-link voltage," IEEE Trans Power Electron, vol. 34, no. 6, pp. 5378–5387, Jun. 2019, doi: 10.1109/TPEL.2018.2866045.

[11] M. Guan, "A series-connected offshore wind farm based on modular dual-active-bridge (DAB) isolated dc–dc converter," IEEE Transactions on Energy Conversion, vol. 34, no. 3, pp. 1422–1431, May 2019, doi: 10.1109/tec.2019.2918200.

[12] F. Rong, G. Wu, X. Li, S. Huang, and B. Zhou, "All-dc offshore wind farm with series-connected wind turbines to overcome unequal wind speeds," IEEE Trans Power Electron, vol. 34, no. 2, pp. 1370–1381, Feb. 2019, doi: 10.1109/TPEL.2018.2834965.

[13] H. J. Bahirat and B. A. Mork, "Operation of dc series-parallel connected offshore wind farm," IEEE Trans Sustain Energy, vol. 10, no. 2, pp. 596–603, Apr. 2019, doi: 10.1109/TSTE.2018.2839712.

[14] H. Zhang, F. Gruson, D. M. F. Rodriguez, and C. Saudemont, "Overvoltage limitation method of an offshore wind farm with dc series-

parallel collection grid," IEEE Trans Sustain Energy, vol. 10, no. 1, pp. 204–213, Jan. 2019, doi: 10.1109/TSTE.2018.2829929.

[15] A. O. Almeida, M. A. Tomim, P. M. Almeida, and P. G. Barbosa, "A control strategy for an offshore wind farm with the generating units connected in series with a VSC-HVDC transmission link," Electric Power Systems Research, vol. 180, Mar. 2020, doi: 10.1016/j.epsr.2019.106121.

[16] G. Guo et al., "Series-connected-based offshore wind farms with full-bridge modular multilevel converter as grid- and generator-side converters," IEEE Transactions on Industrial Electronics, vol. 67, no. 4, pp. 2798–2809, Apr. 2020, doi: 10.1109/TIE.2019.2912777.

[17] R. Zeng, L. Xu, L. Yao, and B. W. Williams, "Design and operation of a hybrid modular multilevel converter," IEEE Trans Power Electron, vol. 30, no. 3, pp. 1137–1146, 2015, doi: 10.1109/TPEL.2014.2320822.

[18] S. Wang, A. M. Massoud, and B. W. Williams, "A T-type modular multilevel converter," IEEE J Emerg Sel Top Power Electron, vol. 9, no. 1, pp. 843–857, 2021, doi: 10.1109/JESTPE.2019.2953007.

[19] G. Guo, K. Zha, J. Zhang, Z. Wang, F. Zhang, and J. Cao, "Grounding fault in series-connection-based offshore wind farms: fault clearance," IEEE Trans Power Electron, vol. 35, no. 9, pp. 9357–9367, Sep. 2020, doi: 10.1109/TPEL.2020.2971640.

[20] P. Lakshmanan, R. Sun, and J. Liang, "Electrical collection systems for offshore wind farms: a review," CSEE Journal of Power and Energy Systems, vol. 7, no. 5. Institute of Electrical and Electronics Engineers Inc., pp. 1078–1092, Sep. 01, 2021. doi: 10.17775/CSEEJPES.2020.05050.

[21] Q. Wei, B. Wu, D. Xu, and N. R. Zargari, "A medium-frequency transformer-based wind energy conversion system used for current-source converter-based offshore wind farm," IEEE Trans Power Electron, vol. 32, no. 1, pp. 248–259, Jan. 2017, doi: 10.1109/TPEL.2016.2524635.

[22] A. O. Almeida, I. F. Lopes, P. M. Almeida, M. A. Tomim, J. A. Passos Filho, and P. G. Barbosa, "Series-dc connection of offshore wind generating units - modeling, control and galvanic isolation.," Electric Power Systems Research, vol. 195, Jun. 2021, doi: 10.1016/j.epsr.2021.107149.

[23] J. Tait, S. Wang, K. Ahmed, and G. P. Adam, "Comparative assessment of four low voltage fault ride through techniques (LVFRT) for wind energy conversion systems (WECSs)," Alexandria Engineering Journal, vol. 61, no. 12, pp. 10463–10476, Dec. 2022, doi: 10.1016/j.aej.2022.04.003.

[24] H. Liu, M. S. A. Dahidah, J. Yu, R. T. Naayagi, and M. Armstrong, "Design and control of unidirectional dc-dc modular multilevel converter for offshore dc collection point: theoretical analysis and experimental validation," IEEE Trans Power Electron, vol. 34, no. 6, pp. 5191–5208, Jun. 2019, doi: 10.1109/TPEL.2018.2866787.

[25] General Electric Company, "HVDC valves power electronics for HVDC schemes," 2019. Accessed: Sep. 20, 2022. [Online]. Available: https://resources.gegridsolutions.com/hvdc/hvdc-valves-brochure

[26] E. Shahriari, F. Gruson, P. Vermeersch, P. Delarue, F. Colas, and X. Guillaud, "A novel dc fault ride through control methodology for hybrid modular multilevel converters in HVDC systems," IEEE Transactions on Power Delivery, vol. 35, no. 6, pp. 2831–2840, Dec. 2020, doi: 10.1109/TPWRD.2020.2998535.

[27] A. Egea-Alvarez, S. Fekriasl, F. Hassan, and O. Gomis-Bellmunt, "Advanced vector control for voltage source converters connected to weak grids," IEEE Transactions on Power Systems, vol. 30, no. 6, pp. 3072–3081, Nov. 2015, doi: 10.1109/TPWRS.2014.2384596.

[28] W. Yang, Q. Song, and W. Liu, "Decoupled control of modular multilevel converter based on intermediate controllable voltages," IEEE Transactions on Industrial Electronics, vol. 63, no. 8, pp. 4695–4706, Aug. 2016, doi: 10.1109/TIE.2016.2549001.

[29] S. Wang, G. P. Adam, A. M. Massoud, D. Holliday, and B. W. Williams, "Analysis and assessment of modular multilevel converter internal control schemes," IEEE J Emerg Sel Top Power Electron, vol. 8, no. 1, pp. 697–719, Mar. 2020, doi: 10.1109/JESTPE.2019.2899794.

[30] G. Guo et al., "HB and FB MMC based onshore converter in series-connected offshore wind farm," IEEE Trans Power Electron, vol. 35, no. 3, pp. 2646–2658, Mar. 2020, doi: 10.1109/TPEL.2019.2929689.

[31] W. Wang, X. Yan, S. Li, L. Zhang, J. Ouyang, and X. Ni, "Failure of submarine cables used in high-voltage power transmission: characteristics, mechanisms, key issues and prospects," IET Generation, Transmission and Distribution, vol. 15, no. 9. John Wiley and Sons Inc, pp. 1387–1402, May 01, 2021. doi: 10.1049/gtd2.12117.

[32] ABB, "ABB wind turbine converters : ACS880, 800 kW to 8 MW," 2018. Accessed: Sep. 20, 2022. [Online]. Available: https://search.abb.com/library/Download.aspx?DocumentID=3AUA0000231755&LanguageCode=en&DocumentPartId=&Action=Launch

[33] Siemens, "The new benchmark for highest availability and maximum energy yield: SINAMICS W180," 2022. https://new.siemens.com/us/en/markets/wind/equipment/energy-generation/wind-converters.html (accessed Sep. 20, 2022).

[34] A. Bensalah, G. Barakat, and Y. Amara, "Electrical generators for large wind turbine: trends and challenges," Energies, vol. 15, no. 18, p. 6700, Sep. 2022, doi: 10.3390/en15186700.

[35] Siemens Gamesa Renewable Technology, "SG 8.0-167 DD offshore wind turbine," 2022. https://www.siemensgamesa.com/products-and-services/offshore/wind-turbine-sg-8-0-167-dd (accessed Sep. 20, 2022).

[36] P. Hou, W. Hu, M. Soltani, and Z. Chen, "Optimized placement of wind turbines in large-scale offshore wind farm using particle swarm optimization algorithm," IEEE Trans Sustain Energy, vol. 6, no. 4, pp. 1272–1282, Oct. 2015, doi: 10.1109/TSTE.2015.2429912.

[37] D. van Hertem, O. Gomis-Bellmunt, and J. Liang, HVDC grids: for offshore and supergrid of the future. IEE, 2016.

[38] Cleaveland / Price Inc., "Aluminum center break switch bulletin DB-126B18," 2022. Accessed: Sep. 20, 2022. [Online]. Available: https://www.cleavelandprice.com/wp-content/uploads/2018/10/No-crop-lines-CP_CBA-VBrochure_3.16.18_FA_LOW-RES.pdf

[39] Siemens Energy, "CPV2/CPV2S circuit switchers and 3AP live-tank breakers." Accessed: Sep. 20, 2022. [Online]. Available: https://assets.siemens-energy.com/siemens/assets/api/uuid:3e08d087-f191-413f-a047-896455a1df37/brochure-cpv2-cpv2s-circuit-switchers-3ap-lt-breakers-us.pdf

[40] Matthias Heidemann, Gregor Nikolic, Armin Schnettler, Ala Qawasmi, Nils Soltau, and Rik W. De Donker, "Circuit-breakers for medium-voltage dc grids," IEEE PES Transmission & Distribution Conference and Exposition, 2016.

[41] X. Xiang et al., "Comparison of cost-effective distances for LFAC with HVAC and HVDC in their connections for offshore and remote onshore wind energy," CSEE Journal of Power and Energy Systems, vol. 7, no. 5, pp. 954–975, Sep. 2021, doi: 10.17775/CSEEJPES.2020.07000.

[42] S. Hardy, K. van Brusselen, S. Hendrix, and D. van Hertem, "Techno-economic analysis of HVAC, HVDC and OFAC offshore wind power connections.," 2019 IEEE Milan PowerTech, 2019.

[43] P. Lundberg, "HVDC light - power from shore," 2016. Accessed: Sep. 20, 2022. [Online]. Available: https://new.abb.com/docs/librariesprovider46/pw2016/seminars/r607-en-abb_hvdc_light_power_from_shore.pdf?sfvrsn=2

[44] P. Bresesti, W. L. Kling, R. L. Hendriks, and R. Vailati, "HVDC connection of offshore wind farms to the transmission system," IEEE Transactions on Energy Conversion, vol. 22, no. 1, pp. 37–43, Mar. 2007, doi: 10.1109/TEC.2006.889624.

James Tait received the first-class B.Eng (Hons) and M.Sc. with distinction degrees in electrical engineering from Edinburgh Napier University, Edinburgh, U.K., and University of Strathclyde, Glasgow, U.K., in 2017 and 2018, respectively. He is currently working toward the Ph.D. degree in the University of Strathclyde. His research interests include wind energy conversion, power electronic converters, and fault resiliency in dc collector networks for offshore wind farms.

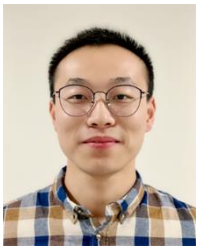

Shuren Wang (S'18) received the first-class honored B.Sc. degree and distinguished M.Sc. degree from Yangzhou University, Yangzhou, China, in 2013 and 2016, respectively. He received the Ph.D. degree from the University of Strathclyde, Glasgow, U.K., in 2020.

Dr. Wang was with Dade Tech, Bosch, and TMR Energy as Engineers. He was a Research Assistant and a Research Associate with the University of Strathclyde, Glasgow, U.K., where he is currently a Research Fellow. He has been a leading researcher in multiple research programs in the fields of power electronics and power systems, and is currently a Co-Principal Investigator (Co-PI) leading an industrially funded research project in the field of integrated renewable energy system development. He is also a contributor for multiple IEEE, IET and Elsevier journals/conferences. His research interests include power electronics, HVDC systems, integration of renewables, converter-dominated grids, and energy storage systems.

Khaled H. Ahmed (M'09–SM'12) received the B.Sc. (first class hons.) and M.Sc. degrees in electrical engineering from Alexandria University, Alexandria, Egypt, in 2002 and 2004, respectively. He received the Ph.D. degree in power electronics applications from the University of Strathclyde, Glasgow, UK, 2008.

Currently, Dr Ahmed is a Reader in Power Electronics at the University of Strathclyde, Glasgow, UK. He is a senior member of the IEEE Power Electronics and Industrial Electronics societies. He has published more than 160 technical papers in refereed journals and conferences as well as a published textbook entitled 'High Voltage Direct Current Transmission: Converters, Systems and DC Grids', a book chapter contribution, and a PCT patent PCT/GB2017/051364. He serves as a Co Editor-in-Chief of Elsevier Alexandria Engineering Journal, and as an Associate Editor of IEEE Open Journal of the Industrial Electronics Society (OJIES), and IEEE Access. His research interests are renewable energy integration, high power converters, offshore wind energy, DC/DC converters, HVDC, and smart grids.